SCIENCE MEETS LIFE

In-situ sequencing of *ABCA7* in Alzheimer disease brain

Lena Duchateau[1,2], Bob Asselbergh[3], Laura Valgaeren[4], Yannick Vermeiren[5,6], Benjamin Pavie[7,8,9], Anne Sieben[5,10], Peter P De Deyn[5,6], Kristel Sleegers[1,2]

[1]Kristel Sleegers Lab, VIB Center for Molecular Neurology, VIB, Antwerp, Belgium, [2]Laboratory of Neurogenetics, Institute Born-Bunge, University of Antwerp, Belgium, [3]Neuromics Support Facility, VIB – UAntwerp Center for Molecular Neurology, Antwerp, Belgium, [4]Faculty of Pharmaceutical, Biomedical and Veterinary Sciences, University of Antwerp, Belgium, [5]Laboratory of Neurochemistry and Behaviour, Institute Born-Bunge, University of Antwerp, Wilrijk, Belgium, [6]Department of Neurology and Alzheimer Research Center, University of Groningen, University Medical Center Groningen, Groningen, The Netherlands, [7]VIB-KU Leuven Center for Brain & Disease Research, Leuven, Belgium, [8]Department of Neurosciences, KU Leuven, Leuven, Belgium , [9]VIB Bio Imaging Core, KU Leuven, Leuven, Belgium , [10]Neurology Department, Gent University Hospital, Gent, Belgium

VIB-UANTWERPEN CENTRUM VOOR MOLECULAIRE NEUROLOGIE

Universiteit Antwerpen

IBB

lena.duchateau@uantwerpen.vib.be

@LenaDuchateau

Background

ABCA7 is one of the most compelling risk genes for Alzheimer's disease (AD) to come out of genome-wide association studies (GWAS). However, it remains unclear what the exact function is of ABCA7, its isoforms and its role in AD pathogenesis. We conducted a pilot study on the use of Cartana's *in-situ* sequencing (ISS) to study spatial expression of *ABCA7* using post-mortem brain samples.

Methods

Brain tissue blocks, obtained from the Brain Bank of the Born-Bung institute, were cryosectioned coronally with a cryomicrotome into 16 µm slices and further stored at -80°C. All equipment was treated with RNaseZAP to prevent RNA degradation. Samples were then sent to CARTANA for library preparation, sequencing and imaging.

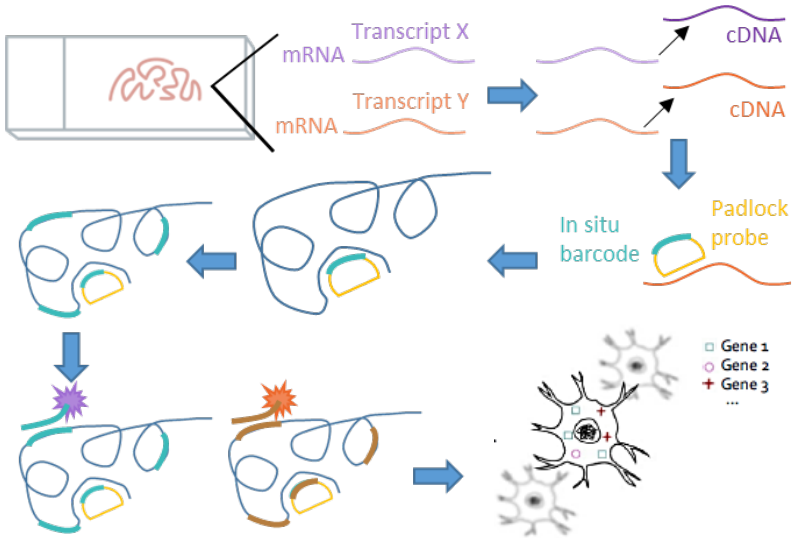

RNA is fixated in the tissue and reverse transcribed *in-situ*. Padlock probes then hybridize to the transcripts of interest and are amplified with rolling circle amplification (RCA). Fluorescence-labeled adaptor probes are hybridized and imaged, creating a tissue map.

Methods

A custom assay was designed including 9 probes for different *ABCA7* isoforms (canonical, intron 6 retention, startcodon at exon 7, exon 19 and exon 30), 8 for AD-related genes of interest (including *APP*, *APOE* and *TREM2*), and 15 probes for cell-type markers (three per cell type; astrocytes, endothelial cells, neurons, oligodendrocytes and microglia). Furthermore, DAPI staining was performed to visualize nuclei. Two types of output data were generated: the coordinates of the nucleus, as determined by DAPI staining, and coordinates of the probes. Using the probe data, we computed probe count per section, tissue and diagnosis. Next, we performed cell segmentation based on DAPI staining using the Watershed method (Fiji script in ImageJ) for all cells and assigned probes to cells for two samples, followed by determination of the number of cells and co-clustering of probes. Finally, we also performed spatial clustering on the data, using Ripley's K in the R package spatstat to study co-clustering.

Study cohort

Sample-ID	Tissue	Diagnosis
Sample 1	BA10, HC, CB	AD
Sample 2	BA10	AD
Sample 3	BA10, HC	AD
Sample 4	BA10, HC	AD
Sample 5	BA10, HC	CON

Results

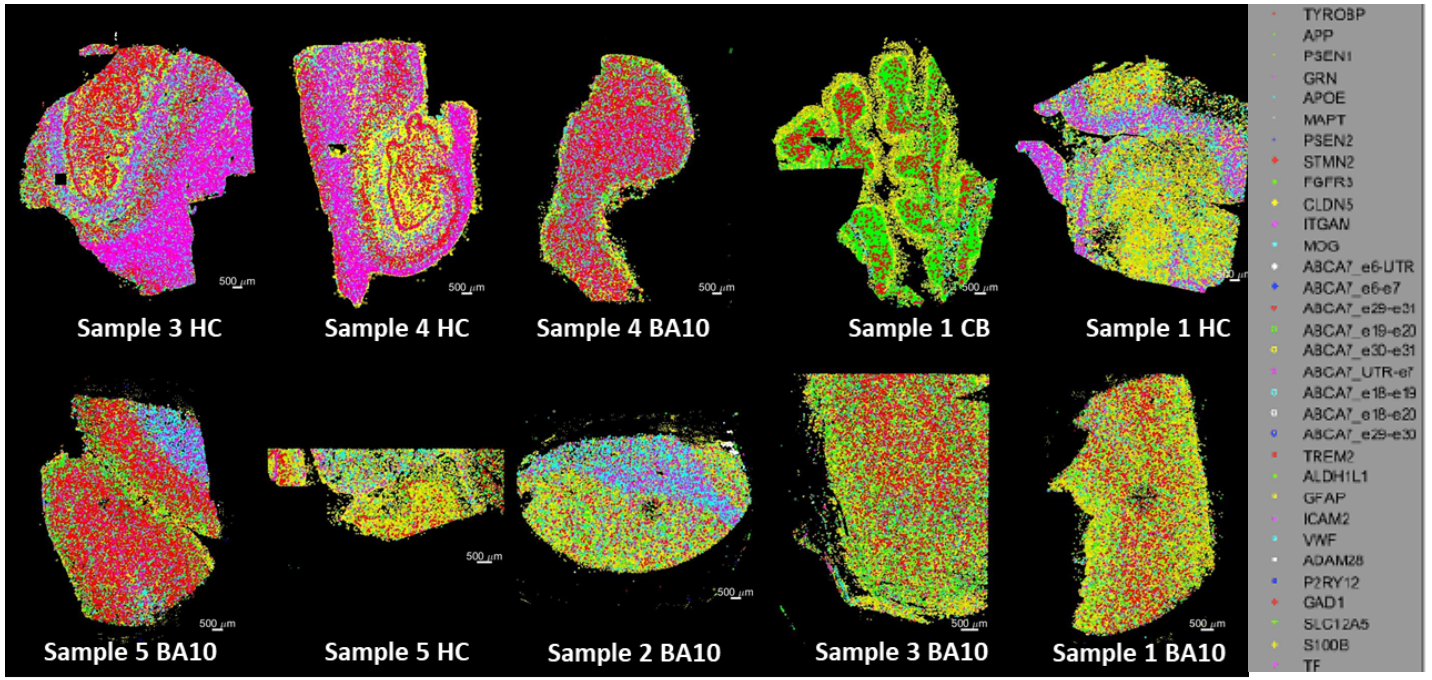

Figure 1: Overview of tissue maps for the different sections, and the probe legend.

Results

Probe data analysis

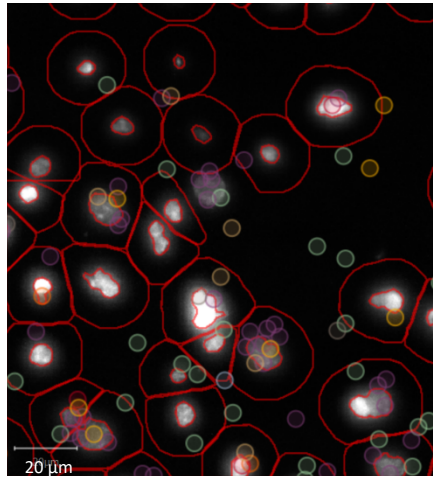

Figure 2: Close-up of sample-3 BA10 with DAPI stains (grey), cell segmentation (red) and probes (green=GFAP, orange=PSEN2, red=APOE, purple=APP, blue=ABCA7). Average density is 1,28 reads per 400 µm²

Probe counts per section were normalized to size, resulting in a density of probe counts. The average number for this was 2.1 ± 2.1 reads per 400 µm² ranging from 0.6 (sample-2 HC) to 7.0 reads per 400 µm² (sample-4 HC), indicating a lot of variation between the sections. Tissues were further divided into subregions where the highest density of probes was found in the fimbria region of the hippocampus (sample-4) and lowest in the white matter of the cerebellum (sample-1). The probe count for the astrocyte marker *GFAP* (green in figure 2) was highest in almost al sections, ranging from 17.4 to 93% of all transcripts, with the exception of the granular layer of the cerebellum (sample-1) (where *SLC12A5* was highest), white matter in sample-5 BA10 (*MOG*), choroid plexus in sample-1 HC (*APP*) and white matter in sample-5 BA10 (*APP*). This emphasizes one drawback we encountered with the data: the probe count was highly dependent on probe sensitivity and thus absolute probe counts are not quantifiable.

Cell segmentation

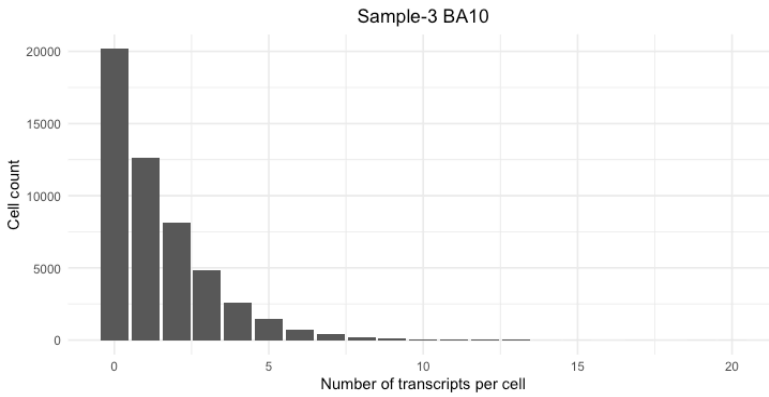

Figure 3: Transcripts per cell in sample-3 BA10

Cell segmentation was performed for all samples, but the probes were only assigned to cells for sample-1 and -3 BA10. The average number of cells per sections is 97,872 ranging from 30,553 to 163,544. Segmented data shows that a majority of cells are empty. On average 46.45% of cells have more than 1 transcript with an average 0.96 ± 1.3 transcript per cell. This sparsity, also seen on figure 2, does complicate some of the downstream analysis.

Results

Comparison methods for co-clustering

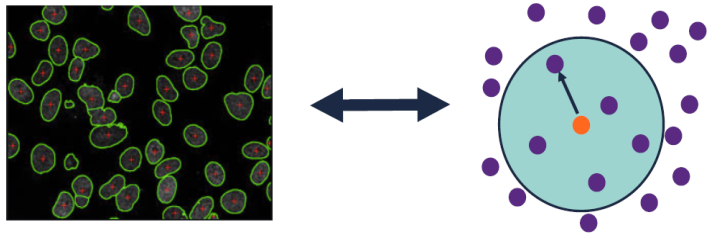

Figure 4: Comparison of sensitivity for co-clustering between cell segmentation (left) and spatial clustering right.

Spatial clustering determines how well data points of a specific type cluster together. A high Kcross value means higher clustering degree.

Co-clustering can be studied with spatial clustering and cell segmentation. To investigate which method is better, we compared their ability to discriminate co-clustering of cell markers of the same cell type (positive pairs) to co-clustering of cell markers of a different cell type (negative pairs). We chose to look at *SLC12A5*, *STMN2* (both neuronal markers), *MOG*, *TF* (both oligodendrocyte markers) and, *ALDH1L1* and *FGFR3* (both astrocytes markers). In each region 10 random regions of a certain size were selected, and for regions with sufficient probe count co-clustering was calculated by determining the odds ratio (OR) (cell segmentation) or Kcross value (Spatial clustering). The smaller the region where discrimination is possible, the higher the sensitivity.

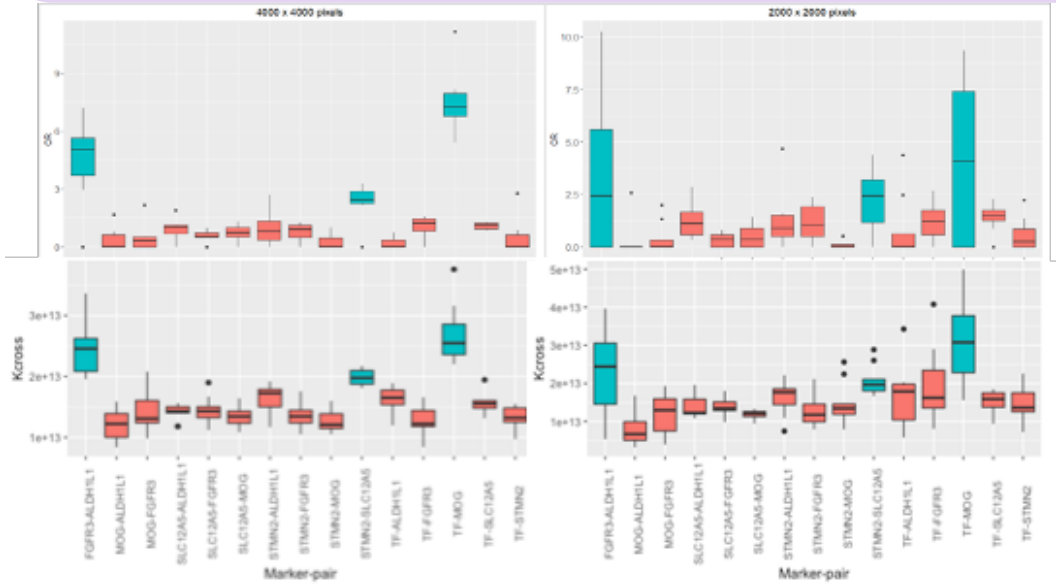

Figure 5: Comparison sensitivity of cell segmentation (up) (8 and 7 regions) and spatial clustering (bottom) (10 regions) for co-clustering discrimination in sample-3 BA10.

Both methods seemed to have a comparable sensitivity with the sensitivity of the methods mostly seeming to depend on quality of the data, such as number of transcripts per cell (cell segmentation) and density (spatial clustering).

Results

ABCA7 expression in subregions

In each section *ABCA7* probes were taken together and expression was normalized against total transcript count. Overall *ABCA7* had highest expression in CB, followed by BA10 and HC with the difference between the last two significant (p=0.05). Expression in controls sections was also slightly higher. For the subregions, *ABCA7* expression is highest in the choroid plexus, followed by the granular layer of the cerebellum.

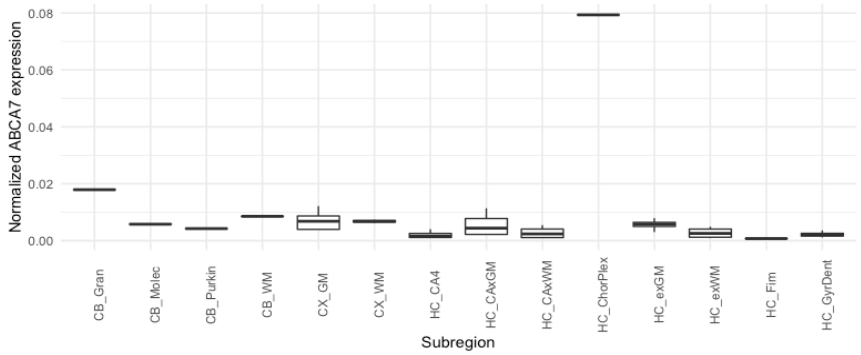

Figure 6: *ABCA7* normalized expression in the different brain subregions.
WM=white matter
GM= grey matter
CA= CA layers (CA1-CA3)
Fim= fimbria
GyrDent= gyrus dentus
ChorPlex=choroid plexus
Gran= granular layer
Molec= molecular layer
Purkin = purkinje cells

Cell type enrichment with segmentation data

Sample	Tissue	OR	Cell-type	Probe	P-value
Sample 1	BA10	1.16 (1.06-1.26)	Neuron	*APP*	$4.99*10^{-3}$
Sample 3	BA10	1.43 (1.39-1.47)	Neuron	*APP*	$1.17*10^{-132}$
Sample 3	BA10	1.35 (1.10-1.64)	Neuron	*ABCA7*	$3.21*10^{-2}$
Sample 3	BA10	1.49 (1.38-1.61)	Neuron	*MAPT*	$3.16*10^{-24}$
Sample 3	BA10	5.54 (2.63-10.55)	Microglia	*TREM2*	$7.08*10^{-6}$

Co-localization of cell-type markers with probes within a cell was calculated using logistic regression in sample-1 and -3 BA10. For sample-1 only *APP* was found to be significantly enriched in neurons, for sample-3 four probes were enriched.

Overall the results of cell type enrichment with segmentation data point out certain flaws of this data mining technique. There is a large number of empty cells and only a limited amount of cells have multiple probes. Moreover, only few probes are significantly enriched in certain cell-types, with only *APP* enrichment found in both sections. Also looking at spatial clustering for cell type enrichment could help overcome this problem.

Results

Cell type enrichment with spatial clustering data

Another way to look at cell type enrichment is by using Kcross and spatial clustering. A higher Kcross value for co-clustering of the transcript of interest with certain cell type marker is indicative of expression in this cell type. Kcross is corrected for regions size.

Figure 7: Spatial clustering of *ABCA7, APP* and *TREM2* with cell type markers with different colors for different sections.

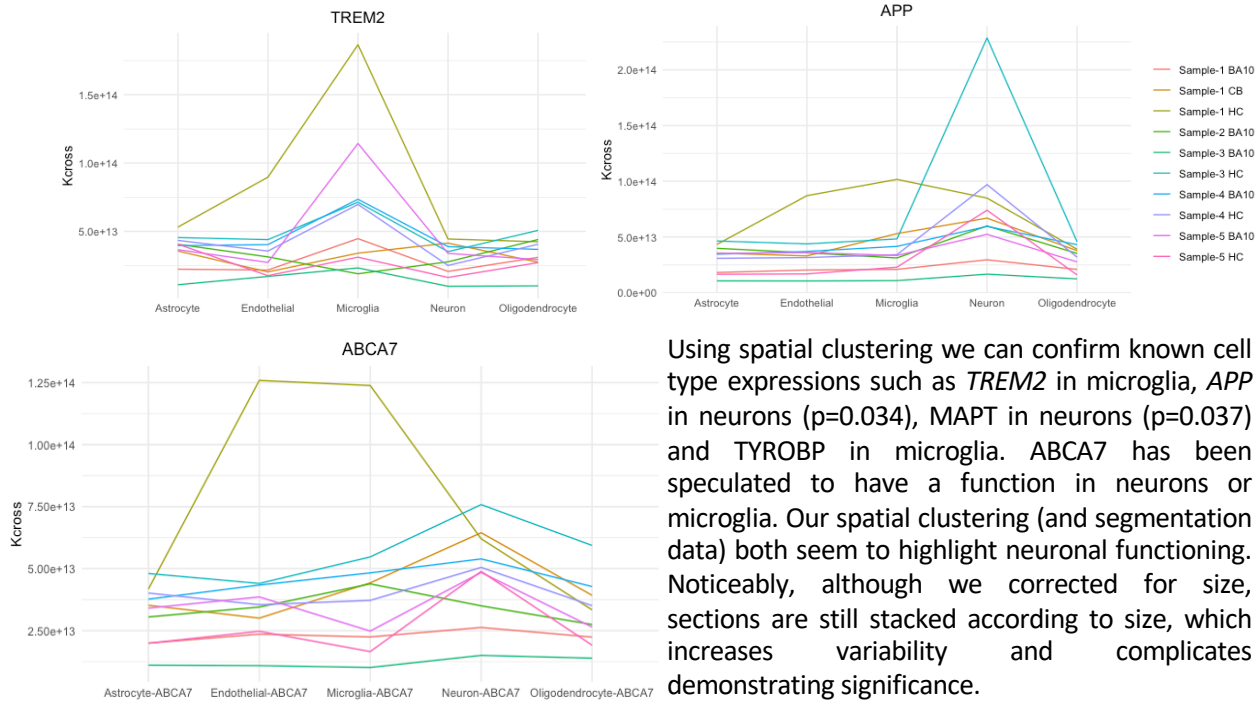

Using spatial clustering we can confirm known cell type expressions such as *TREM2* in microglia, *APP* in neurons (p=0.034), MAPT in neurons (p=0.037) and TYROBP in microglia. ABCA7 has been speculated to have a function in neurons or microglia. Our spatial clustering (and segmentation data) both seem to highlight neuronal functioning. Noticeably, although we corrected for size, sections are still stacked according to size, which increases variability and complicates demonstrating significance.

Conclusion

Although this technique, and its analysis, still need further optimization and fine-tuning, our data proves it could be a useful technique to study AD-related genes. Moreover, spatial clustering also proves to be a promising technique to study this type of data. Our results highlight that probe design is a critical step, and pinpoint neurons and the choroid plexus as being of specific interest for further *ABCA7* studies.